International Journal of Engineering and Geosciences
https://dergipark.org.tr/en/pub/ijeg
e-ISSN 2548-0960

Studying urbanization pattern in Sambalpur City during 1992-2042 using CA-ANN, and Markov-Chain model

Avijit Bag[1], Arabinda Sharma*[1], Sudhakar Pal[1]

[1] Gangadhar Meher University, School of Geography, India, bagavijit79@gmail.com, arbind_78@rediffmail.com, palsudhakar61@gmail.com

Cite this study: Bag, A., Sharma, A., & Pal, S. (2024). Studying urbanization pattern in Sambalpur City during 1992-2042 using CA-ANN, and Markov-Chain model. International Journal of Engineering and Geosciences, 9 (3), 356-367

https://doi.org/ 10.26833/ijeg.1452005

Keywords
Land use/land cover
CA-ANN
Markov- Chain
Urban Sprawl
Random Forest Model

Research Article

Received: 13.03.2024
Revised: 20.04.2024
Accepted: 23.04.2024
Online Published: 17.11.2024

Abstract

Models of land use/land cover (LULC) are crucial for assessing changes in LULC, forecasting land use needs, and providing guidance for appropriate land use planning and management, especially in urban areas. Urban sprawl is one of the main causes of the erratic variation in LULC around the globe. In this study, we used the CA-ANN and Markov-Chain models to analyze the LULC simulation based on LULC patterns from previous decades as well as the directional changes of urban expansion in Sambalpur city. We used the random forest (RF) model and Landsat imagery to prepare LULC maps for the years 1992, 2002, 2012, and 2022 for better classification accuracy. The result showed that the overall accuracy and kappa values were 94.24%, 89%, 94%, and 90% and 0.92, 0.80, 0.90, and 0.85, respectively, for the selective years. Based on the transition matrix model (1992–2012), the LULC map of the year 2022 was obtained and validated, and subsequently, LULC maps for the years 2032 and 2042 were predicted with a Kappa value of 94.97% and 93.24%, respectively. The findings indicate that the largest proportion of bare land underwent conversion within the settlement area, with the highest degree of sprawl observed in the northwestern direction and 4-kilometer buffer zones. These findings define current and future patterns in LULC and offer vital information for planning and sustainable land use management in Sambalpur city.

1. Introduction

Globally, the rate of urbanization has increased during the previous century, significantly changing the natural landscape. Currently, around 55% of people on the planet reside in cities, and by 2050, that number is expected to rise to 68% [1]. The consequences of urbanization are very clear, especially in developing nations where urban planning is frequently inadequate. According to the 2011 census [2], India, for example, had a notable 2.76% increase in its urban population between 2001 and 2011. Due to the pressure of high population densities, major Indian cities like Delhi, Mumbai, Chennai, Kolkata, and Pune are dealing with serious environmental and socioeconomic difficulties [3]. As a result, the swift and uncontrolled expansion of urban regions causes significant alterations in the surrounding landscapes.

The term land use describes how land is utilized, such as for cultivation, amusement, or habitat for wildlife. The physical material that makes up Earth's surface is referred to as land cover. This includes both naturally occurring features like vegetation, water bodies, and bare soil as well as man-made features like residential infrastructure, highways, and agricultural fields. [4–7]. The LULC collectively established a crucial element of the environmental systems [8]. The expansion of industry, agriculture, and human settlements stands as a primary driver for the transformation of natural areas in developing nations [8, 9]. Fast urban expansion across various regions globally has led to significant changes in LULC types. Numerous research studies have documented how urban growth has led to the encroachment of surrounding landscape features, including wetlands, agricultural land, water bodies, forests, and shrublands [10–14].

LULC mapping emerges as a pivotal method for studying global ecology, environmental studies, and societal planning and development, facilitating the monitoring of the world's functions. Previous studies

highlight LULC mapping's primary role in examining biodiversity, built-up areas, farmland, water quality, and more, contributing significantly across various domains [15–20]. It provides valuable assistance in sustainable land management, environmental assessment, natural resource management, climate change analysis, disaster planning and response, as well as urban and regional planning [21]. The impact of Land Use and Land Cover (LULC) change can vary depending on several factors, but in general, it can have significant environmental, social, and economic consequences. Some of the key impacts include habitat loss and fragmentation [22], climate change [23], soil degradation [24], change of livelihood [25], etc. LULC mapping provides valuable insights into the Earth's surface dynamics, supporting informed decision-making, sustainable land management, and environmental conservation efforts.

The methods for studying the LULC mechanism have rapidly evolved, incorporating techniques such as spatiotemporal modeling, transition potential modeling, and simulation [26]. Ensuring greater accuracy in LULC mapping, including the prediction of future land changes, is crucial for effective planning purposes [28]. Remote sensing data can be utilized to analyze and monitor LULC changes over time [29]. Numerous studies have utilized Landsat imagery and Sentinel-2 imagery to classify Land Use and Land Cover (LULC) maps, aiming to enhance the comprehension of trends, predict LULC changes [30–33], and detect sprawl [34, 35]. Furthermore, several scholars utilize the Google Earth Engine (GEE) to address this issue [35]. By using satellite imagery and other remote sensing techniques, researchers and land managers can assess the impact of human activities on land use, track deforestation or urban expansion, and evaluate the effectiveness of land management strategies for the development of socio-economical and environmental phenomena.

When assessing future LULC scenarios under potential circumstances, simulation models of LULC transition and prediction are useful and repeatable methods [36]. Many researchers have proposed that the past, present, and future studies of LULC depend upon various models, such as Dinamica [37], FLUS [36], CA-ANN [37], Markov Chain Model [8], and SERGoM [38]. Cellular automata (CA) is a popular technique for simulating land-use change processes because it can accurately depict nonlinear, spatially stochastic processes. Of all those models, the Markov Chain and CA-ANN models are more realistic and helpful techniques for predicting and simulating the LULC change [8, 29].

The researcher employed the MOLUSCE model and multispectral satellite data to forecast Land Use and LULC changes in various locations. This approach also includes the analysis of alternative land uses and the computation of their transfer rates [39]. Asia Air Survey developed an open-source MOLUSCE plugin for QGIS 2.0 and above, which incorporates popular algorithms like artificial neural networks (ANNs), multi-criteria evaluation (MCE), weights of evidence (WoE), logistic regression (LR), and the Monte Carlo cellular automata (CA) model [37, 40]. In this study, the CA-ANN model was utilized due to its efficacy in comprehending land-use systems and their dynamics when combined with other methodologies [41]. It's crucial to forecast future land changes for effective planning and management of land use and land cover [28].

The rapid growth and concentration of the population in Sambalpur City have resulted in a notable horizontal expansion of urban space, commonly known as urban sprawl [42]. Scholars suggest that this urban expansion occurs in various directions from the city center toward its periphery, influenced by socioeconomic factors like rivers, slopes, high land, industry, roads, and markets, among others [42, 43]. Detecting directional sprawl is crucial for effective urban planning and management. In summary, the research conducted by the mentioned authors indicates that LULC changes pose a complex challenge, and a thorough understanding of spatial system components is essential. The Markov-based cellular automata model proves valuable for prediction, although enhancing simulation accuracy may require additional factors [44]. Additionally, Landsat imagery, utilized with the GEE, provides a dependable LULC map and a comprehensive view of the study area.

Given the rapid urbanization and population growth in Sambalpur city over the past few decades, the study hypothesizes that there will be significant spatiotemporal changes in LULC from 1992 to 2022, with a continued trend of urban expansion and increased urban sprawl. Furthermore, we anticipate that these changes will continue into the future, leading to further alterations in LULC patterns by 2032 and 2042.

At this outset, the present study was carried out with the following major objectives: (i) to analyze the spatiotemporal LULC change from 1992 to 2022 using multispectral satellite images; (ii) to forecast the LULC change trend for the years 2032 and 2042; and (iii) to find out the directional urban sprawl of Sambalpur City. The framed objective for the study area is of great significance, as it will aid planners and policymakers in designing cities and in the development and planning of various policies for the community.

2. Materials and Methods

2.1. Study area

Sambalpur city, a major central city of Sambalpur district and the 5th largest city of Odisha, India, is located on the eastern bank of the Mahanadi River (21° 24' 59.73" N to 21° 31' 33.18"N and 83° 55' 5.40" E to 84° 02' 10.21"E) (Figure 1). In this study, we selected this city that is bounded by its surrounding villages and has an area of about 81.56 km^2. This city has a tropical climate, and the mean yearly temperature observed in this city has been recorded at 27°C (en.climate-data.org). Here, rapid urbanization has been observed in the last few decades. According to the 2011 census of India, the total population of this city is 184,000, and the population density is 4,405. The continuous change of LULC in this city has led to urban ecosystem degradation, causing vegetation covers, water bodies, and bare land loss and increasing the built-up area. Under the current

enactment, this city has been protected by the Sambalpur-Burla-Hirakud Master Plan [45].

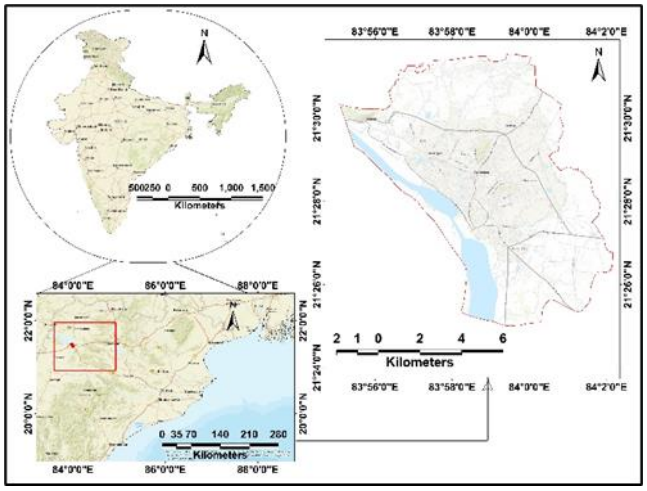

Figure 1. Location map of the study area

Sambalpur is experiencing rapid urbanization and significant land use/land cover (LULC) changes, making it an ideal location to investigate urban sprawl dynamics and their impacts. Additionally, Sambalpur's geographical and socioeconomic characteristics, such as its location in an ecologically sensitive region and emerging urban development challenges, provide a unique context for studying LULC patterns and their implications for sustainable land use management. Sambalpur's strategic significance as a hub for trade, commerce, and infrastructure development in the region emphasizes the need to comprehend its land-use and land-cover dynamics.

2.2. Data source

In this study, we use Landsat images from 1992 to 2022 in 10-year intervals; these were collected from the USGS Landsat (8, 7, and 5) Collection 2 Tier 1 TOA Reflectance in Google Earth Engine (GEE). We selected the TOA reflectance material as a function of variations in (1) solar zenith angles, (2) spectral band differences, and (3) Earth-to-Sun distances at different times of the year. Its reflectance algorithm eliminates the explanatory outcomes relating to high solar radiation [46]. The NASA SRTM Digital Elevation 30m dataset was used for slope and DEM. The road network was collected from the Open Street Dataset for the mapping of distance to the road with the help of the ArcGIS 10.8 toolbox. We have also collected the population data from the official website of the Registrar General and Census Commissioner of India (https://censusindia.gov.in/census.website/) to understand the urban growth and intensity of urbanization throughout the decade. Using ground samples gathered via field surveys and Google Earth Pro (for 1992 and 2022) allowed for the validation of the prepared LULC maps (for 2022).

2.3. Methodology

The methodology adopted is presented in Figure 2. It basically comprises a number of sub-procedures such as LULC map preparation, accuracy assessment, simulation of future LULC maps, and directional urban sprawl analysis.

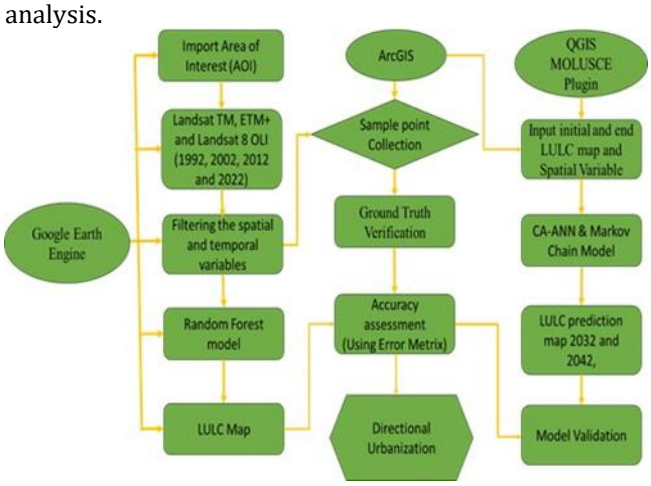

Figure 2. Methodological flowchart

2.3.1. LULC classification

The study area's LULC was divided into four major categories: built-up area, vegetation cover, bare land, and water bodies. All the LULC maps were made in different years based on the Simple Random Forest Model (RF) using Landsat 5 (TM), Landsat 7 (ETM+), and Landsat 8 (OLI/TIRS) datasets with 30m resolution.

In order to classify LULC, we first import the region of interest (ROI) and the above-mentioned Landsat data into the GEE code editor. Then we bound the ROI with the satellite image and also clipped the ROI from the satellite image. After completing all the processes, we collected the training samples, comprising around 4% of the total area evenly distributed within the city boundary, for the various classes. Furthermore, to handle high-dimensional data sets, we combine the various bands with the various classes and input the RF method, which provides the maximum accuracy for LULC and remote sensing classifications [47, 48].

2.3.2. Accuracy assessment

For an accurate and effective examination of LULC change, accuracy assessment for individual classification is crucial [49–51]. The accuracy assessment is conducted using statistical measures like producer's and user's accuracies, kappa coefficients, and error matrices. The accuracy of four LULC maps from 1992, 2002, 2012, and 2022 was assessed using 400 (100 for each year and 25 for each class) reference points collected randomly from the Google Earth platform. Based on the comparison of LULC observed and predicted for reference points, a confusion matrix is created. The method is most frequently used to evaluate the accuracy of land cover maps [52–54], as it allows the computation of the Producer Accuracy (PA), User Accuracy (UA), and Overall Accuracy (OA). Kappa coefficient (k.) was also used to calculate the degree to which the extracted value and real value agree. The following equations are used to calculate accuracy and the kappa coefficient [34, 55, 56].

$$PA = = \frac{Number\ of\ correctly\ classified\ pixels}{Total\ number\ of\ reference\ pixels} \quad \text{.....(1)}$$

$$UA = \frac{Number\ of\ correctly\ classified\ pixels}{Total\ number\ of\ classified\ pixels} \quad (2)$$

$$OA = \frac{Sum\ of\ all\ correctly\ classified\ pixels}{Total\ number\ of\ pixels\ observed} \quad (3)$$

$$\hat{k} = \frac{N\sum_{i=0}^{n} X_{ii} - \sum_{i=0}^{n} X_{i+} \cdot X_{+i}}{N^2 - \sum_{i=0}^{n} X_{i+} \cdot X_{+i}} \quad (4)$$

2.3.3. Simulation of LULC changes

Modules of Land Use Change (MOLUSCE), an open-source model based on cellular automata that were incorporated into QGIS software as a plug-in, was utilized for LULC modeling [26, 25, 45, 57]. Additionally, it analyzes the circumstances of alternative land uses and computes their transfer rates using cross-tabulation methods, utility modules, and algorithmic modules [36]. Here, we use the CA-ANN Markov Chain model, because it is a useful tool for comprehending land-use systems and the underlying dynamics of those systems when paired with other approaches [38]. The chosen model is a very effective non-linear data mining tool, suitable as a global parametric model for modeling LULC [57]. In this study, we generated the change detection map from 1992–2002, 2002–2012, and 2012–2022, which helped to analyze the CA-ANN model. Slope, DEM, and distance to the road map were all spatial variables used for the higher accuracy of the prediction map. Using the CA-ANN Markov Chain model, we generated the LULC prediction map for the year 2032 using classified LULC images from 2012 and 2022 and the 2042 predicted map generated from 2022 and 2032 LULC images. Using Kappa statistics for model calibration and validation, creating a change map, and assessing the connection between the spatial variables were important phases in the modeling process [58].

2.3.4. Directional urban sprawl

The assessment of urban sprawl can be done in different ways that engage computational and equational methods; these are Diversity, Density, and Spatial Compactness Measurement (SCM) [32, 45, 59]. But in this study, the concept was simple and was just visualization and calculation of the decadal growth of built-up areas in different directions, which indicates the sprawl rate of the city. Here, the spatiotemporal change of the built-up area was divided into 8 directions, and each direction was divided into 4 buffer zones with a 2 km interval from the city's center.

In ArcGIS, the study area is defined, temporal data is imported, and pertinent data layers are compiled to construct directed urban sprawl. Differences in land cover are computed, density surfaces are created, and changes in land use and cover over time are analyzed. Tools such as the Raster Calculator are utilized to identify areas experiencing urban expansion. The length of a possible corridor study and the distance between current metropolitan regions and future growth zones are determined. Symbology and labeling are implemented to provide clarity when creating maps and visualizations to represent the results. The relationship between the direction of urban sprawl and variables like the expansion of built-up areas is analyzed by performing spatial statistics.

3. Results and Discussion

This study examines the urban growth and patterns observed from 1992 to 2022, focusing on Land Use and Land Cover (LULC) changes. It presents the decadal trend and intensity of urban LULC changes, along with the directional shift of the built-up area expanding from the city center towards its periphery. Furthermore, the study includes future predictions based on LULC simulations for the years 2032 and 2042.

3.1. LULC classification

Time Series of LULC maps with class compositions is a straightforward and easiest method to show the dynamic of the visual earth's surface in different decades. Here, the LULC map was classified into four different land classes: water bodies (river, channel, wetland, pond, etc.), vegetation covers (forest, bushes, grasses, etc.), barren land (agricultural land, bare land, open land grassland, etc.), and built-up areas (settlement area, industrial area, market area, constructed surface, etc.), which are shown in Table 1. The LULC maps showing the spatial distribution of various LULC classes during the years 1992, 2002, 2012, and 2022 are given in Figure 3. Based on the statistical assessment of accuracy, the OA for these maps was 94.24%, 89%, 94%, and 90%, and the kappa coefficient ($\hat{k}$) was 0.92, 0.80, 0.90, and 0.85, respectively.

In 1992, the water bodies showed 7.61%, but in 2002, they increased because of seasonal changes in precipitation, and they gradually decreased in 2012 (4.05 sq km) and 2022 (2.66 sq km) after 2002. The vegetation cover fluctuated during the first decade (1992–2002) due to seasonal variations and other human activities, but it was fairly constant during the entire study session.

Table 1. LULC area (sq km) 1992-2022 with percentage

Classes	Area (sq km)				Area (%)			
	1992	2002	2012	2022	1992	2002	2012	2022
Water Bodies	6.21	6.67	4.05	2.66	7.61	8.18	4.96	3.26
Vegetation	11.45	9.68	10.02	10.94	14.04	11.87	12.29	13.41
Bare Land	59.62	53.89	49.28	41.57	73.10	66.07	60.42	50.97
Built-up Area	4.28	11.32	18.21	26.39	5.25	13.88	22.33	32.36
Total	81.56	81.56	81.56	81.56	100	100	100	100

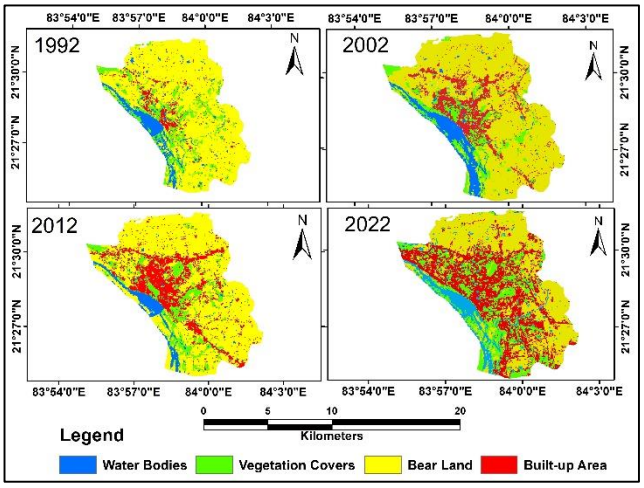

Figure 3. The study area's LULC map

In 1992, the vegetation cover was 14.04%, followed by 11.87%, 12.29%, and 13.41% in 2002, 2012, and 2022, respectively. The bare land consistently decreases due to the continuous increase of the built-up area, signifying rapid urbanization, as shown in Figure 3.

Therefore, the bare land reflected 73.10% during the year 1992, but it decreased in 2002 (66.07%), 2012 (60.42%), and 2022 (50.97%), respectively. Built-up areas increased due to the high increase in population. During 1992, the built-up area was 4.28 sq km (5.28%), followed by 11.32 sq km (13.88%), 18.22 sq km (14.78%), and 26.39 sq km (32.36%) during the study period. People moved into an area in search of greater economic prospects, which resulted in the development of towns and the expansion of infrastructure. The need for public facilities, utilities, and transportation networks is rising along with the population and economy. The LULC has therefore undergone substantial modifications, with vegetated land, water bodies, and other LULC kinds being transformed into areas for residential or commercial development, thus expanding the area of built-up land [60]. However, the decrease in green and open space brought about by urbanization poses a danger to several Sustainable Development Goals (SDG) indicators of the United Nations (UN) and results in environmental imbalance [42]. The Sustainable Cities and Communities (SDG 11) and Life on Land (SDG 15) SDGs are directly affected by the study's findings. Specifically, the study's analysis of urban sprawl, land use changes, and their implications in Sambalpur city aligns with SDG 11's indicators, such as the ratio of land consumption rate to population growth rate (Indicator 11.3.1) and the proportion of urban solid waste disposed of in an environmentally sound manner (Indicator 11.6.1). The study's findings about Sambalpur's land use and degradation patterns additionally endorse SDG 15's indicator on the percentage of degraded land to total land area (Indicator 15.3.1). These relationships emphasize the study's importance in addressing important sustainability issues and guiding sustainable urban development and land use management strategies.

3.2. Decadal change of LULC

Both natural and anthropogenic processes exhibit land surface dynamics, but anthropogenic causes have the greatest potential to alter the urban land surface. The socio-economic drivers behind the Land Use and Land Cover (LULC) change in Sambalpur City, Odisha, are multifaceted. These drivers encompass factors such as rapid population growth, urbanization, industrialization, agricultural practices, infrastructure development, government policies, land tenure systems, and socio-cultural dynamics. Together, these drivers influence land use decisions, leading to shifts in LULC patterns over time and impacting the city's socio-economic landscape. Table 2 represents the percentage of the land surface transformation from the prior year to the current year.

Table 2. Decadal Change Percentage of LULC

Classes	1992-2002 % of Change	2002-2012 % of Change	2012-2022 % of Change	2022-2032 % of Change	2032-2042 % of Change
Water Bodies	7.40	-39.34	-34.27	-7.67	-13.60
Vegetation	-15.44	3.48	9.15	-3.71	3.44
Bare Land	-9.61	-8.55	-15.64	-4.18	-3.22
Built-up Area	164.29	60.92	44.89	8.74	4.23

Due to the expansion of habitation, the area covered by vegetation decreased by 15.44% and the area of bare land decreased by 9.61% between 1992 and 2002; nonetheless, over this decade, the area covered by water bodies grew by 7.40%. Since 2000, Sambalpur has experienced rapid urbanisation as a result of population growth and the expansion of large-scale industries in the surrounding area. The administrative boundary used here was the boundary of the newly established Sambalpur Municipal Corporation (SMC) in the year 2013. It encompasses the former Sambalpur Municipality, Burla NAC, Hirakud NAC, and 63 neighbouring villages. In addition, several infrastructure and other development projects were proposed to meet the basic needs of the newly formed SMC's residents. As a result, natural land features such as vegetation, bare land (primarily fallow and waste land), and water bodies have been the most impacted by these developments. However, the local urban authority and the state government have consistently tried to nullify the negative impact.

Consequently, the water bodies and barren land steadily decreased, and the built-up area rose between the decades of 2002–2012 and 2012–2022 and also the predicted years, as shown in Figure 4. The anticipated 2022–2032 and 2032–2042 decades show such outcomes. The growth of built-up land in the future loosens its accelerated increasing trend due to the non-availability or limited availability of suitable land for infrastructure development. In such a situation, the city has to look toward the surrounding villages to accommodate the growing population of the city.

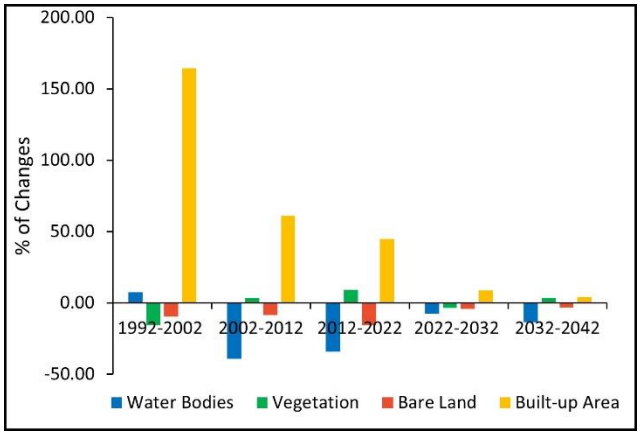

Figure 4. Percentage of area change in different decades

3.3. Transition matrix

When examining temporal changes within a group of LULC categories, the transition matrix is crucial [61]. The proportions of pixels shifting from one land use/cover to another are displayed in the transition matrix. It also helps in understanding the driving forces behind the prevailing LULC change.

According to Table 3, the maximum number of water bodies that changed into vegetation covers during the 1992–2002 decade was 0.15 sq km; the maximum number of vegetation covers that changed into bare land was 0.46 sq km; the maximum number of bare lands that changed into the built-up area was 0.32 sq km; and the maximum number of built-up areas that changed into bare land was 0.29 sq km. Similarly, the majority of water bodies and vegetation cover were turned into barren land between 2002 and 2012. (0.20 sq km and 0.41 sq km), and the bare ground was then transformed into the built-up area (0.85 sq km). In contrast, the highest amount of bare land, water bodies, and vegetation cover that were converted into built-up areas between 2012 and 2022 were 0.24, 0.25, and 0.24 sq km, respectively, while 0.12 sq km of built-up area was converted into vegetation cover.

Table 3. Transition matrix for the decade of 1992-2002, 2002-2012, and 2012-2022

Years	Classes	Water Bodies	Vegetation	Bare Land	Built-up area
1992-2002	Water Bodies	0.74	0.15	0.08	0.02
	Vegetation	0.13	0.46	0.28	0.13
	Bare Land	0.01	0.05	0.82	0.32
	Built-up area	0.00	0.07	0.29	0.63
2002-2012	Water Bodies	0.21	0.07	0.20	0.01
	Vegetation	0.08	0.51	0.41	0.10
	Bare Land	0.10	0.00	0.80	0.85
	Built-up area	0.03	0.00	0.00	0.51
2012-2022	Water Bodies	0.12	0.02	0.12	0.24
	Vegetation	0.05	0.92	0.03	0.25
	Bare Land	0.03	0.14	0.59	0.24
	Built-up area	0.02	0.12	0.00	0.74

3.4. Directional urban sprawl

Unplanned and spontaneous urban growth from the city center towards the surrounding region is known as urban sprawl [59]. There are many causes to grow of the city toward its periphery. These include rapid population influx, lack of effective urban planning strategies, inadequate infrastructure development, socioeconomic factors driving migration to urban areas, absence of land use regulations, and geographical features influencing settlement patterns. These interrelated variables cause urban areas to grow out of control in certain directions, posing problems like increased demand for natural resources, environmental deterioration, and ineffective land use management. Figure 5 reveals the directional change of urban sprawl in 1992, 2002, 2012, and 2022. Here, we selected a total of 8 directions with a 2 km interval from the city center (Laxmi Talkies Square) to its surroundings.

Table 4 indicates that in 1992, the urban growth extension was most significant in the NW direction, covering 1.76 square kilometers. Similarly, the N, E, NE, SE, S, W, and SW directions encompassed 0.91, 0.54, 0.49, 0.47, 0.11, 0.10, and 0.04 square kilometers, respectively. In 2002, the NW direction expanded to 3.98 square kilometers, whereas the NE, N, SE, E, S, W, and SW directions expanded to 2.95, 2.90, 2.11, 1.49, 0.23, 0.14, and 0.08 square kilometers, respectively. Furthermore, the maximum urban sprawl occurred in the NW direction in 2012 and 2002, covering areas of 5.57 and 7.85 square kilometers, respectively, while W and SW exhibited minimal expansion, as depicted in Figure 6a.

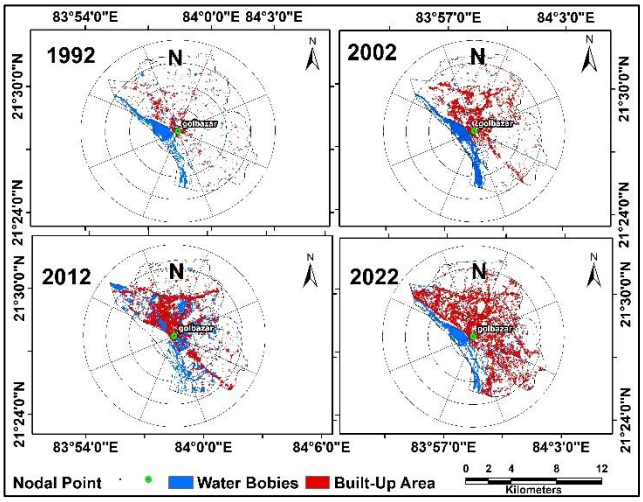

Figure 5. Directional change map on urban sprawl in Sambalpur city from 1992-2022

The urban area has grown similarly in all directions except the west and southwest, which indicates that there is currently a river there. The city has little to no space for development on the other sides of the river due to the non-availability of suitable land for development. A vast portion of these come under the flood plain area of the river, and hence the river itself acts as the boundary of the city. However, an unanticipated increase in urban expansion has occurred in the northwest due to the availability of a variety of facilities, including low-cost housing, plenty of open space, and transportation and communication infrastructure.

Table 4. Direction and distance-wise change of urban expansion area

Years	Direction Wise Area (sq km)								Distance (km) Wise Area (sq km)			
	E	N	NE	NW	S	SE	SW	W	2 km	4 km	6 km	8 km
1992	0.54	0.91	0.49	1.76	0.11	0.47	0.04	0.10	1.24	0.90	0. 82	0.21
2002	1.49	2.90	2.95	3.98	0.23	2.11	0.08	0.14	4.10	5.02	2.82	0.95
2012	2.54	3.07	3.06	5.57	0.25	3.46	0.09	0.16	3.64	8.88	3.43	2.25
2022	4.28	4.38	4.42	7.85	0.95	5.25	0.10	0.20	4.86	11.30	8.51	2.78

According to Figure 6. b, the spread of urban area was the greatest year-round in the 4 km buffer zone, followed by 6 km, 2 km, and 8 km, respectively. In 1992, the buffer zone of 2 km (1.24 sq km) experienced the highest rate of urban growth. Other buffer zones measured 0.90, 0.82, and 0.21 sq km, respectively. Similarly, the maximum urban growth for the year 2002 occurred in the 4 km (5.02 sq km) buffer zone; similar trends continued in 2012 (8.88 sq km) and 2022 (11.30 sq km). In 2012, the areas that fall under the 2km, 6km, and 8 km buffer zones were 3.64, 3.43, and 2.25 sq. km; in 2022, the areas that fall under the 2km, 6km, and 8 km buffer zones are 4.86, 8.51, and 2.78 sq km.

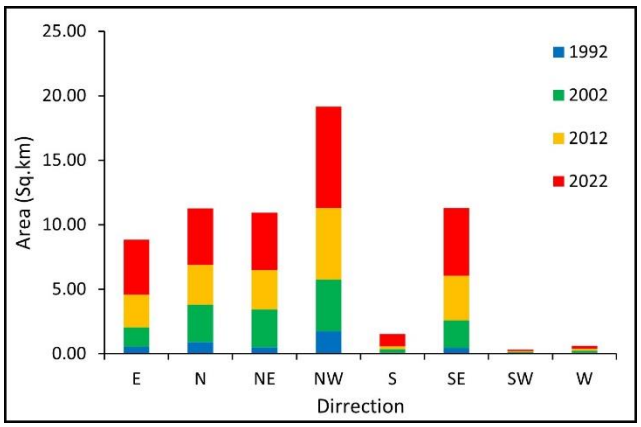

Figure 6. (a) Direction-wise change of built-up area

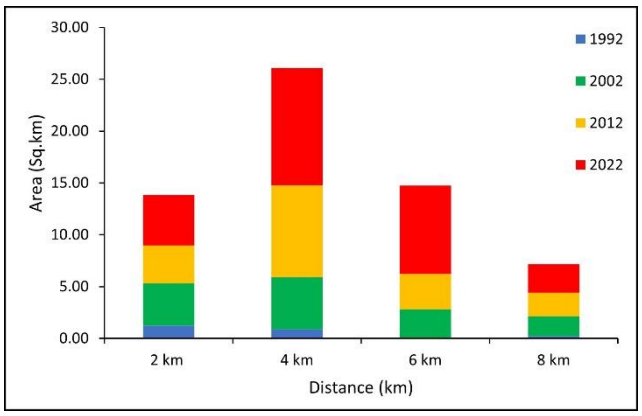

Figure 6. (b) Distance-wise built-up area

3.5. Transition potential modeling (TPM)

In this study, the forecasted LULC map for 2022, 2032, and 2042 was predicted using the Artificial Neural Network (Multilayer Perception) technique. We have used a random sampling method with a sample size of 1000 for implementing the Artificial Neural Network (ANN) model in the context of TPM. The learning curve of the model is depicted in Figure 7. From 2012 to 2022, for the implementation of the ANN (Layer Protection) model, we selected parameters including 10 hidden layers, a learning rate of 0.001, and a maximum of 100 iterations. When the actual (observed) and predicted LULC maps for 2022 were validated, the kappa coefficient was found to be sufficiently high. It resulted in an overall accuracy of 0.00145, a minimum validation overall error of 0.16292, and a validation kappa coefficient of 0.85481.

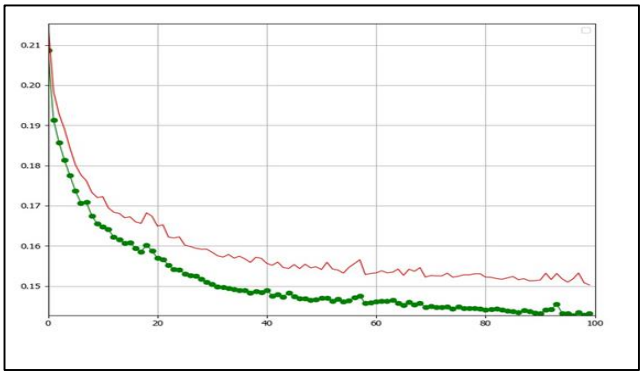

Figure 7. Neural network learning curve

The green curve in Figure 7 displays the actual value of the LULC map, while the red curve indicates the expected value. Since the two carvings are so close to one another, the projected LULC map's accuracy and inaccuracy are at their maximum and minimum here.

3.6. Simulation of future LULC changes

The MOLUSCE is a helping tool to predict the LULC map depending on the two successive future LULC maps of 2032 and 2042. Here, we selected the initial year 2012 and final year 2022 maps for the predicted map in the years 2022, 2032, and 2042. According to Figure 8, the results showed that the actual and predicted maps for 2022 were very accurate. Where the difference between actual and predicted water bodies is 0.49 sq km, vegetation covers 0.38 sq km, bare land is 0.66 sq km, and built-up area is 0.20 sq km, respectively.

Hence, the projected map of 2032 indicated that the built-up area is continuously growing and the water bodies and bare land are decreasing thoroughly, but the vegetation cover is nearly the same as shown in Figure 8, which follows in the year 2042. The vegetation covers showed nearly 13% of all the predicted years, and the water bodies in 2032 and 2042 were 2.46% and 2.13%, respectively. Therefore, the bare land was converted into the built-up area, where in 2032 and 2042, the bare land showed 49.61% and 48.02%, respectively. On the other hand, the built-up area in 2032 and 2042 was found to be 35.46% and 36.96%, as shown in Table 5. The probability of the various land use classes from 2032 to 2042 is displayed in Figure 8.

Indeed, population growth and economic development are widely recognized as primary drivers of built-up expansion in this urban area, as supported by numerous studies [5, 62]. The identical result was discovered by [63], the forecasted maps for Sambalpur, Odisha, between 2032 and 2042 revealed a notable uptrend in urbanized areas, accompanied by a simultaneous decline in agricultural lands. Throughout the study, the results also showed a tendency to decline in agricultural and water-covered areas. The state of Sambalpur City experienced a continual rise in urban expansion, according to the modeling of LULC maps from 2032 to 2042.

Table 5. Simulation of LULC changes of 2032 and 2042

	Simulated Area (Sq km)			Simulated Area (%)		
Classes	2022	2032	2042	2022	2032	2042
Water Bodies	2.17	2.01	1.73	2.66	2.46	2.13
Vegetation	10.56	10.17	10.52	12.95	12.47	12.89
Bare Land	42.23	40.47	39.17	51.78	49.61	48.02
Built-up Area	26.60	28.92	30.15	32.61	35.46	36.96
Total	81.56	81.56	81.56	100	100	100

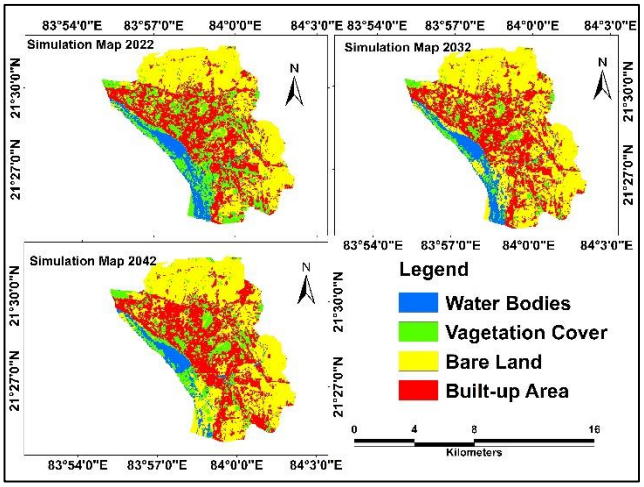

Figure 8. Prediction and reference map for 2022, 2032 and 2042

3.7. Model validation

After conducting change detection, transition analysis, and prediction, we proceeded to evaluate transitions in the Land Use and Land Cover (LULC) map during the validation process. The CA-Markov model was validated by comparing the simulated and real LULC maps for 2032 and 2042 in Figure 8, yielding 2032 values for % of correctness, Kappa (overall), Kappa (histo), and Kappa (loc). Furthermore, the accuracy of this study was demonstrated by its percentage of correctness (94.97), kappa variation location (0.99), kappa (histo) (0.93), and kappa (overall) (0.92). Similarly, in the map of 2042, the percentage of correctness was 93.24, kappa variation's location (0.97), kappa (histo) (0.92), and kappa (overall) (0.91). It indicates that the result of the future LULC map was very accurate, and this map should be used as a reference for future urban planning and development.

4. Conclusion

The primary goal of this research is to forecast the LULC based on the last three decades employing the Markov Chain model, the CA-ANN, and the direction of urban expansion in Sambalpur City. Based on the result, we concluded that the LULC has significantly changed in the last three decades. Generally, we found that Landsat

Image and GEE Computing provided LULC maps for the years 1992, 2002, 2012, and 2022 with overall accuracies and Kappa values, which were 94.24%, 89%, 94%, 90%, and 0.92, 0.80, 0.90, and0.85, respectively. Based on the transition probability matrix, we found that the maximum area of bare land converted into a built-up area in all four decades, which will be continued in future i.e., during 2032 and 2042. We also found that the NW direction showed maximum outgrowth along the road, and the W and SW directions were minimal. The CA-ANN model run also showed the percentage of correctness for the years 2032 and 2042 at 94.97% and 93.24%, respectively. It indicates the usefulness of the model for forecasting LULC. In this work, we simulated and forecasted landscape changes exclusively using physical factors; however, other socio-economic, development policies, immigration, migration, and climatic factors may also affect landscape patterns. Policies for development and agriculture can also be connected to support sustainable urbanization, which can be accommodated in future research. Despite these limitations, the present outcome provided valuable insight into the changing urbanization and LULC pattern in Sambalpur City.

The study evaluated LULC changes in the city of Sambalpur using the CA-ANN, Markov-Chain, and Random Forest models. It pointed up drawbacks including the potential for simplicity in the modeling of urban development processes and the bias-introducing dependence on data availability and quality. Better data gathering and model refinement are essential for making more precise projections of future LULC patterns. Future studies could enhance LULC modeling by integrating various data sources, like satellite imagery and socioeconomic data. Including climate change variables in these models can provide insights into how environmental factors influence urban sprawl and land use decisions. Incorporating these advancements can lead to more robust and sustainable land use management strategies for cities like Sambalpur.

Acknowledgement

The 1st author is thankful to the University Grants Commission, New Delhi for providing with fellowship for carrying out the research work.

Author contributions

Avijit Bag: Methodology, Validation, Resources, Formal analysis, Investigation, Writing – Original draft **Arabinda Sharma:** Conceptualization, Methodology, Resources, Supervision, Reviewing and editing **Sudhakar Pal:** Conceptualization, Methodology, Resources, Supervision, Reviewing and editing.

Conflicts of interest

The authors declare no conflicts of interest.

References

1. Zhang, X. Q. (2016). The trends, promises and challenges of urbanisation in the world. Habitat International, 54(13), 241–252. https://doi.org/10.1016/j.habitatint.2015.11.018
2. United Nations, (2018). 68% of the world population projected to live in urban areas by 2050. Retrived June 17, 2023, from https://www.un.org/development/desa/en/news/population/2018-revision-of-world-urbanization-prospects.html
3. Sridhar, K. S. (2021). Urbanization and COVID-19 Prevalence in India. Regional Science Association International, 2(July 2020), 493–505. https://doi.org/10.1111/rsp3.12503
4. Mishra, V. N., & Rai, P. K. (2016). A remote sensing aided multi-layer perceptron-Markov chain analysis for land use and land cover change prediction in Patna district (Bihar), India. Arabian Journal of Geosciences, 9(4). https://doi.org/10.1007/s12517-015-2138-3
5. Uddin, M. S., Mahalder, B., & Mahalder, D. (2023). Assessment of Land Use Land Cover Changes and Future Predictions Using CA-ANN Simulation for Gazipur City Corporation, Bangladesh. Sustainability (Switzerland), 15(16). https://doi.org/10.3390/su151612329
6. Baig, M. F., Mustafa, M. R. U., Baig, I., Takaijudin, H. B., & Zeshan, M. T. (2022). Assessment of Land Use Land Cover Changes and Future. Water, 1–17. Retrieved from https://doi.org/ 10.3390/w14030402
7. Saputra, M. H., & Lee, H. S. (2019). Prediction of land use and land cover changes for North Sumatra, Indonesia, using an artificial-neural-network-based cellular automaton. Sustainability (Switzerland), 11(11), 1–16. https://doi.org/10.3390/su11113024
8. Khwarahm, N. R., Najmaddin, P. M., Ararat, K., & Qader, S. (2021). Past and future prediction of land cover land use change based on earth observation data by the CA–Markov model: a case study from Duhok governorate, Iraq. Arabian Journal of Geosciences, 14(15), 1–14. https://doi.org/10.1007/s12517-021-07984-6
9. Jat, M. K., Garg, P. K., & Khare, D. (2008). Monitoring and modelling of urban sprawl using remote sensing and GIS techniques. International Journal of Applied Earth Observation and Geoinformation, 10(1), 26–43. https://doi.org/10.1016/j.jag.2007.04.002
10. Forkuor, G., & Cofie, O. (2011). Dynamics of land-use and land-cover change in Freetown, Sierra Leone and its effects on urban and peri-urban agriculture - a remote sensing approach. International Journal of Remote Sensing, 32(4), 1017–1037. https://doi.org/10.1080/01431160903505302
11. Araya, Y. H., & Cabral, P. (2010). Analysis and modeling of urban land cover change in Setúbal and Sesimbra, Portugal. Remote Sensing, 2(6), 1549–1563. https://doi.org/10.3390/rs2061549
12. Mundia, C., & Murayama, Y. (2010). Modeling spatial processes of urban growth in african cities: A case study of nairobi city. Urban Geography, 31(2), 259–272. https://doi.org/10.2747/0272-3638.31.2.259
13. Haregeweyn, N., Fikadu, G., Tsunekawa, A., Tsubo, M., & Meshesha, D. T. (2012). The dynamics of urban expansion and its impacts on land use/land cover change and small-scale farmers living near the urban

fringe: A case study of Bahir Dar, Ethiopia. Landscape and Urban Planning, 106(2), 149–157. https://doi.org/10.1016/j.landurbplan.2012.02.016
14. Fenta, A. A., Yasuda, H., Haregeweyn, N., Belay, A. S., Hadush, Z., Gebremedhin, M. A., & Mekonnen, G. (2017). The dynamics of urban expansion and land use/land cover changes using remote sensing and spatial metrics: The case of Mekelle city of northern Ethiopia. International Journal of Remote Sensing, 38(14), 4107–4129. https://doi.org/10.1080/01431161.2017.1317936
15. Natarajan, K., Latva-Käyrä, P., Zyadin, A., & Pelkonen, P. (2016). New methodological approach for biomass resource assessment in India using GIS application and land use/land cover (LULC) maps. Renewable and Sustainable Energy Reviews, 63, 256–268. https://doi.org/10.1016/j.rser.2016.05.070
16. Gibril, M. B. A., Bakar, S. A., Yao, K., Idrees, M. O., & Pradhan, B. (2017). Fusion of RADARSAT-2 and multispectral optical remote sensing data for LULC extraction in a tropical agricultural area. Geocarto International, 32(7), 735–748. https://doi.org/10.1080/10106049.2016.1170893
17. Li, H., Wang, C., Zhong, C., Zhang, Z., & Liu, Q. (2017). Mapping typical urban LULC from Landsat imagery without training samples or self-defined parameters. Remote Sensing, 9(7), 1–23. https://doi.org/10.3390/rs9070700
18. Prasad, N., & Das, T. (2019). Impact of land use and land cover on aquatic macrophyte community composition in small streams: A case study from cachar district of assam in northeast India. Indian Journal of Ecology, 46(2), 363–370.
19. Whyte, A., Ferentinos, K. P., & Petropoulos, G. P. (2018). A new synergistic approach for monitoring wetlands using Sentinels -1 and 2 data with object-based machine learning algorithms. Environmental Modelling and Software, 104, 40–54. https://doi.org/10.1016/j.envsoft.2018.01.023
20. Tolentino, F. M., & de Lourdes Bueno Trindade Galo, M. (2021). Selecting features for LULC simultaneous classification of ambiguous classes by artificial neural network. Remote Sensing Applications: Society and Environment, 24(May), 100616. https://doi.org/10.1016/j.rsase.2021.100616
21. Thenkabail, P. S., Schull, M., & Turral, H. (2005). Ganges and Indus River basin land use/land cover (LULC) and irrigated area mapping using continuous streams of MODIS data. Remote Sensing of Environment, 95(3), 317–341. https://doi.org/10.1016/j.rse.2004.12.018
22. Sobhani, P., Esmaeilzadeh, H., Barghjelveh, S., Sadeghi, S. M. M., & Marcu, M. V. (2022). Habitat integrity in protected areas threatened by lulc changes and fragmentation: A case study in Tehran Province, Iran. Land, 11(1). https://doi.org/10.3390/land11010006
23. Martín-Arias, V., Evans, C., Griffin, R., Cherrington, E. A., Lee, C. M., Mishra, D. R., … Rosado, S. (2022). Modeled Impacts of LULC and Climate Change Predictions on the Hydrologic Regime in Belize. Frontiers in Environmental Science, 10(April), 1–16. https://doi.org/10.3389/fenvs.2022.848085
24. Kidane, M., Bezie, A., Kesete, N., & Tolessa, T. (2019). The impact of land use and land cover (LULC) dynamics on soil erosion and sediment yield in Ethiopia. Heliyon, 5(12), e02981. https://doi.org/10.1016/j.heliyon.2019.e02981
25. kullo, E. D., Forkuo, E. K., Biney, E., Harris, E., & Quaye-Ballard, J. A. (2021). The impact of land use and land cover changes on socioeconomic factors and livelihood in the Atwima Nwabiagya district of the Ashanti region, Ghana. Environmental Challenges, 5(May), 100226. https://doi.org/10.1016/j.envc.2021.100226
26. Verburg, P. H., Schot, P. P., Dijst, M. J., Veldkamp, A., Verbürg, P. H., Schot, P. P., … Veldkamp, A. (2016). Land use change modelling: current practice and research priorities Linked references are available on JSTOR for this article: Land use change modelling: current practice and research priorities. Source: GeoJournal GeoJoumal, 61(4), 309–324. Retrieved from http://www.jstor.org/stable/41147951%0Ahttp://www.jstor.org/stable/41147951?seq=1&cid=pdf-reference#references_tab_contents%0Ahttp://about.jstor.org/terms
27. Alshari, E. A., & Gawali, B. W. (2022). Modeling Land Use Change in Sana'a City of Yemen with MOLUSCE. Journal of Sensors, 2022. https://doi.org/10.1155/2022/7419031
28. Abbas, Z., Yang, G., Zhong, Y., & Zhao, Y. (2021). Spatiotemporal change analysis and future scenario of lulc using the CA-ANN approach: A case study of the greater bay area, China. Land, 10(6). https://doi.org/10.3390/land10060584
29. Abd El-Kawy, O. R., Rød, J. K., Ismail, H. A., & Suliman, A. S. (2011). Land use and land cover change detection in the western Nile delta of Egypt using remote sensing data. Applied Geography, 31(2), 483–494. https://doi.org/10.1016/j.apgeog.2010.10.012
30. Fallati, L., Savini, A., Sterlacchini, S., & Galli, P. (2017). Land use and land cover (LULC) of the Republic of the Maldives: first national map and LULC change analysis using remote-sensing data. Environmental Monitoring and Assessment, 189(8). https://doi.org/10.1007/s10661-017-6120-2
31. Pirotti, F., Sunar, F., & Piragnolo, M. (2016). Benchmark of machine learning methods for classification of a Sentinel-2 image. International Archives of the Photogrammetry, Remote Sensing and Spatial Information Sciences - ISPRS Archives, 41(July), 335–340. https://doi.org/10.5194/isprsarchives-XLI-B7-335-2016
32. Nguyen, H. T. T., Doan, T. M., Tomppo, E., & McRoberts, R. E. (2020). Land Use / Land Cover Mapping Using Multitemporal Sentinel-2 Imagery and Four Classification. Remote Sens, 12, 1–27. Retrieved from www.mdpi.com/journal/remotesensing
33. Haldar, S., Mandal, S., Bhattacharya, S., & Paul, S. (2023). Dynamicity of land use/land cover (LULC): An analysis from peri-urban and rural neighbourhoods of Durgapur Municipal Corporation (DMC) in India.

Regional Sustainability, 4(2), 150–172. https://doi.org/10.1016/j.regsus.2023.05.001
34. Magidi, J., & Ahmed, F. (2019). Assessing urban sprawl using remote sensing and landscape metrics: A case study of City of Tshwane, South Africa (1984–2015). Egyptian Journal of Remote Sensing and Space Science, 22(3), 335–346. https://doi.org/10.1016/j.ejrs.2018.07.003
35. Mahdavifard, M., Ahangar, S. K., Feizizadeh, B., Kamran, K. V., & Karimzadeh, S. (2023). Spatio-Temporal monitoring of Qeshm mangrove forests through machine learning classification of SAR and optical images on Google Earth Engine. International Journal of Engineering and Geosciences, 8(3), 239–250. https://doi.org/10.26833/ijeg.1118542
36. Han, H., Yang, C., & Song, J. (2015). Scenario simulation and the prediction of land use and land cover change in Beijing, China. Sustainability (Switzerland), 7(4), 4260–4279. https://doi.org/10.3390/su7044260
37. Liu, X., Wei, M., & Zeng, J. (2020). Simulating urban growth scenarios based on ecological security pattern: A case study in quanzhou, china. International Journal of Environmental Research and Public Health, 17(19), 1–19. https://doi.org/10.3390/ijerph17197282
38. Theobald, D. M. (2005). Landscape patterns of exurban growth in the USA from 1980 to 2020. Ecology and Society, 10(1). https://doi.org/10.5751/ES-01390-100132
39. Hakim, A. M. Y., Baja, S., Rampisela, D. A., & Arif, S. (2019). Spatial dynamic prediction of landuse / landcover change (case study: Tamalanrea sub-district, makassar city). IOP Conference Series: Earth and Environmental Science, 280(1). https://doi.org/10.1088/1755-1315/280/1/012023
40. Çubukçu, E. A., Demir, V., & Sevimli, M. F. (2023). Modeling of annual maximum flows with geographic data components and artificial neural networks. International Journal of Engineering and Geosciences, 8(2), 200–211. https://doi.org/10.26833/ijeg.1125412
41. Muhammad, R., Zhang, W., Abbas, Z., Guo, F., & Gwiazdzinski, L. (2022). Spatiotemporal Change Analysis and Prediction of Future Land Use and Land Cover Changes Using QGIS MOLUSCE Plugin and Remote Sensing Big Data: A Case Study of Linyi, China. Land, 11(3). https://doi.org/10.3390/land11030419
42. Alshari, E. A., & Gawali, B. W. (2021). Development of classification system for LULC using remote sensing and GIS. Global Transitions Proceedings, 2(1), 8–17. https://doi.org/10.1016/j.gltp.2021.01.002
43. Mandal, S., Kundu, S., Haldar, S., Bhattacharya, S., & Paul, S. (2020). Monitoring and Measuring the Urban Forms Using Spatial Metrics of Howrah City, India. Remote Sensing of Land, 4(1–2), 19–39. https://doi.org/10.21523/gcj1.20040103
44. Verma, R., & Garg, P. K. (2021). Spatio-temporal land use change analysis in directional zones of Lucknow City, India. International Archives of the Photogrammetry, Remote Sensing and Spatial Information Sciences - ISPRS Archives, 44(M–3), 181–186. https://doi.org/10.5194/isprs-archives-XLIV-M-3-2021-181-2021
45. Hamad, R., Balzter, H., & Kolo, K. (2018). Predicting land use/land cover changes using a CA-Markov model under two different scenarios. Sustainability (Switzerland), 10(10), 1–23. https://doi.org/10.3390/su10103421
46. Pal, S., Sharma, A., & Parida, R. (2023). Status of Green and Open Space in Changing Urban Landscape - A Case Study of Sambalpur City. In A. Sharma & P. N. Sinha (Eds.), Geographical Approaches fior Sustainable Society and Environment (1st ed., pp. 236–251). Kunal Books, New Delhi.
47. Liu, C., Li, W., Zhu, G., Zhou, H., Yan, H., & Xue, P. (2020). Land use/land cover changes and their driving factors in the northeastern Tibetan plateau based on geographical detectors and Google Earth engine: A case study in Gannan prefecture. Remote Sensing, 12(19). https://doi.org/10.3390/RS12193139
48. Ritu, S. M., Sarkar, S. K., & Zonaed, H. (2023). Prediction of Padma River bank shifting and its consequences on LULC changes. Ecological Indicators, 156(October), 111104. https://doi.org/10.1016/j.ecolind.2023.111104
49. Khan, A., & Sudheer, M. (2022). Machine learning-based monitoring and modeling for spatio-temporal urban growth of Islamabad. Egyptian Journal of Remote Sensing and Space Science, 25(2), 541–550. https://doi.org/10.1016/j.ejrs.2022.03.012
50. Butt, A., Shabbir, R., Ahmad, S. S., & Aziz, N. (2015). Land use change mapping and analysis using Remote Sensing and GIS: A case study of Simly watershed, Islamabad, Pakistan. Egyptian Journal of Remote Sensing and Space Science, 18(2), 251–259. https://doi.org/10.1016/j.ejrs.2015.07.003
51. Mosammam, H. M., Nia, J. T., Khani, H., Teymouri, A., & Kazemi, M. (2017). Monitoring land use change and measuring urban sprawl based on its spatial forms: The case of Qom city. Egyptian Journal of Remote Sensing and Space Science, 20(1), 103–116. https://doi.org/10.1016/j.ejrs.2016.08.002
52. Mostafa, E., Li, X., Sadek, M., & Dossou, J. F. (2021). Monitoring and forecasting of urban expansion using machine learning-based techniques and remotely sensed data: A case study of Gharbia governorate, Egypt. Remote Sensing, 13(22). https://doi.org/10.3390/rs13224498
53. Sidi Almouctar, M. A., Wu, Y., Kumar, A., Zhao, F., Mambu, K. J., & Sadek, M. (2021). Spatiotemporal analysis of vegetation cover changes around surface water based on NDVI: a case study in Korama basin, Southern Zinder, Niger. Applied Water Science, 11(1), 1–14. https://doi.org/10.1007/s13201-020-01332-x
54. Kamusoko, C., & Aniya, M. (2008). Hybrid classification of Landsat data and GIS for land use/cover change analysis of the Bindura district, Zimbabwe. International Journal of Remote Sensing, 30(1), 97–115. https://doi.org/10.1080/01431160802244268

55. Gwet, K. (2016). EuroHeartCare 2016. European Journal of Cardiovascular Nursing, 15(1_suppl), S1–S115. https://doi.org/10.1177/1474515116634263
56. Santhosh, L. G., & Shilpa, D. N. (2023). Assessment of LULC change dynamics and its relationship with LST and spectral indices in a rural area of Bengaluru district, Karnataka India. Remote Sensing Applications: Society and Environment, 29(November 2022), 100886. https://doi.org/10.1016/j.rsase.2022.100886
57. El-Tantawi, A. M., Bao, A., Chang, C., & Liu, Y. (2019). Monitoring and predicting land use/cover changes in the Aksu-Tarim River Basin, Xinjiang-China (1990–2030). Environmental Monitoring and Assessment, 191(8), 1–18. https://doi.org/10.1007/s10661-019-7478-0
58. Mubako, S., Nnko, H. J., Peter, K. H., & Msongaleli, B. (2022). Evaluating historical and predicted long-term land use/land-cover change in Dodoma Urban District, Tanzania: 1992–2029. Physics and Chemistry of the Earth, 128(April), 103205. https://doi.org/10.1016/j.pce.2022.103205
59. Mehriar, M., Masoumi, H., & Mohino, I. (2020). Urban sprawl, socioeconomic features, and travel patterns in Middle East countries: A case study in Iran. Sustainability (Switzerland), 12(22), 1–20. https://doi.org/10.3390/su12229620
60. Haldar, S., Mandal, S., Bhattacharya, S., & Paul, S. (2023). Regional Sustainability Dynamicity of Land Use / Land Cover (LULC) An analysis from peri-urban and rural neighbourhoods of Durgapur Municipal Corporation (DMC) in India. Regional Sustainability, 4(2), 150–172. https://doi.org/10.1016/j.regsus.2023.05.001
61. Guha, S., & Govil, H. (2022). Seasonal impact on the relationship between land surface temperature and normalized difference vegetation index in an urban landscape. Geocarto International, 37(8), 2252–2272. https://doi.org/10.1080/10106049.2020.1815867
62. Wu, R., Li, Z., & Wang, S. (2021). The varying driving forces of urban land expansion in China: Insights from a spatial-temporal analysis. Science of the Total Environment, 766, 142591. https://doi.org/10.1016/j.scitotenv.2020.142591
63. Ahmad, S., Paulami, Y., Kansara, B. B., & Kalubarme, M. H. (2020). Monitoring land use changes and its future prospects using cellular automata simulation and artificial neural network for Ahmedabad city, India. GeoJournal, 5. https://doi.org/10.1007/s10708-020-10274-5

© Author(s) 2024. This work is distributed under https://creativecommons.org/licenses/by-sa/4.0/